Grating micro-dot patterned light guide plates for LED backlights

Seung Ryong Park, Oh Jang Kwon, Dongho Shin, and Seok-Ho Song

BK21 Center, Department of Physics, Hanyang University,
Mt. 17, Hengdang-Dong, Sungdong-Gu, Seoul, Korea
shsong@hanyang.ac.kr

Hong-Seok Lee and Hwan Young Choi

LCD Optics & Material PT, Display Device & Material Lab.,
Samsung Advanced Institute of Technology, Mt. 14-1, Nongseo-Dong, Giheung-Gu, Yongin-Si, Gyeonggi-Do, Korea

Abstract: A novel LED backlight unit implementing a light guide plate (LGP) with a two-dimensional array of grating micro-dots is proposed. By optimizing grating-vector orientations of local gratings and applying suitable grating-depth modulation in the array, taking into consideration of the radiation pattern of the LED source, uniform out-coupled light distribution within a narrow luminance angle was achieved without recognizable hot spots. Such a light guide plate was fabricated using a dot-matrix holographic interferometer setup and a UV embossing replication. Fabricated polycarbonate LGP showed ~62% intensity uniformity within ~8^o and ~20^o luminance angles in two main directions.

OCIS codes: (050.1970) Diffractive optics; (220.4000) Microstructure fabrication.

References and links

1. M. Parikka, t. Kaikuranta, P. Laakkonen, J. Tauyanen, J. Tervo, M. Honkanen, M. Kuittnen, and J. Turunen, "Deterministic diffractive diffusers for displays," Appl. Opt. **40**, 2239-2246 (2001).
2. J. M. Teijido, H. P. Herzig, and R. Dandlinger, "Diffraction properties of volume holographic diffusers," Proc. SPIE **2774,** 747-756 (1996).
3. A. Horibe, M. Baba, E. Nihei, and Y. Koike, "High Efficiency and High Visual Quality LCD Backlighting System," SID **29**, 153-156 (1998).
4. J. M. Teijido, H. P. Herzig, and R. Dandlinger, "Design of a non-conventional illumination system using a scattering light pipe," Proc. SPIE **2951,** 146-155 (1996).
5. S. I. Ochiai, "Light guide plate and light guide plate assembly utilizing diffraction grating," US Patent **5703667** (1997).
6. S. Nam, M. G. Lee, J. H. Kim, J. H. Min, J. S. Choi, S. M. Lee, and H. Y. Choi, "Hologram based light-guide plate for LCD-backlights," IDW **01** (2001).
7. M. G. Lee, H. Y. Choi, J. H. Min, J. S. Choi, J. H. Kim, and S. M. Lee, "Optical characteristics of holographic light-guide plate for LCD," Eurodisplay **2002**, 343-346 (2002).
8. C.-K. Lee, J. Wu, S.-L. Yeh, C.-W Tu, Y.-A. Han, E. Liao, L. Chang, I.-E. Tsai, H.-H. Lin, J. Hsieh, and J. Lee, "Optical configuration and color-representation range of a variable-pitch dot matrix holographic printer," Appl. Opt. **39**, 40-53 (2000).
9. M. G. Moharam and T. K. Gaylord, "Diffractin analysis of dielectric surface-relief gratings," J. Opt. Soc. Am**. 72**, 1385-1392 (1982).
10. M. G. Moharam and T. K. Gaylord, "Three-dimensional vector coupled-wave analysis of planar grating diffraction," J. Opt. Soc. Am **73**, 1105-1112 (1983).
11. M. Neviere, Electromagnetic theory of gratings, R. Petei Ed., Springer Verlag, Berlin (1980).
12. R. Magnusson, Z. S. Liu, D. Wawro, P. P. Young, and D. Shin, "Waveguide-grating coupler for illumination of photonic antennas," Proc. SPIE **3075**, 101-108 (1997).
13. P. Nussbaum, I. Philipoussis, A. Husser, and H. P. Herzig, "Simple technique for replication of micro-optical elements," Opt. Eng. **37** 1804–8 (1998).

#78558 - $15.00 USD Received 2 January 2007; revised 15 February 2007; accepted 27 February 2007

1. Introduction

Liquid Crystal Display (LCD) is one of the most widely used flat-panel display in multimedia devices such as mobile phones, PDAs, PMPs, car navigation systems, digital video cameras, and computer monitors. Current LCD display requires cost effectiveness, low-power consumption, light weight, slim size, and high image quality. In order to satisfy these, high efficiency, slim, high uniformity, and low cost backlight unit (BLU) is required. Additionally, light-emitting diodes (LEDs) are beginning to replace conventional cold cathode fluorescent lamps (CCFLs) as light sources for LCD backlight units due to their desirable characteristics such as a large color gamut, color temperature adjustability, long lifetime, and environmental safety (i.e. mercury free). Compared with CCFL (line source) BLUs, LED-based BLUs suffer from luminance non-uniformity problems such as propagating-light line patterns and hot-spots as LEDs are point-like sources [1]. Various approaches to extract light from BLU have been proposed [2-4]. However, these scattering approaches are suffered by low intensity uniformity with undesirable hot spots due to limited controllability in out-coupling light. An approach that provides controllable light extraction from the LGP is to utilize diffraction gratings [1, 5-7]. The diffractive LGP approach can provide a high efficiency, uniform light distribution with a slim BLU size. Additionally, backlight illumination can be confined in a narrow luminance angle. This makes the diffractive LGP a cost effective solution as functional sheets such as prism sheets can be eliminated from conventional BLU systems.

In this paper, a novel LED backlight unit implementing an LGP having a two-dimensional array of grating micro-dots is presented. By optimizing grating-vector orientations of local gratings and applying suitable grating-depth modulation in the array, taking into account of the radiation pattern of the LED source, uniform out-coupled light distribution within a narrow luminance angle was achieved without recognizable hot spots near the LED source or light-propagation-line pattern. Parikka et al.[1] proposed a similar approach of controlling the grating-vector orientation and a grating fill-factor modulation scheme using long-period (~2.5 μm) gratings fabricated by e-beam lithography and hot embossing replication process. We used submicron-period grating dots utilizing flexible and cost effective dot-matrix holographic lithography [8] and UV embossing replication to achieve the uniformity and directionality in the extracted radiation.

2. Device design and simulation

The grating micro-dot patterned LGP under study is schematically illustrated in Fig. 1(a).

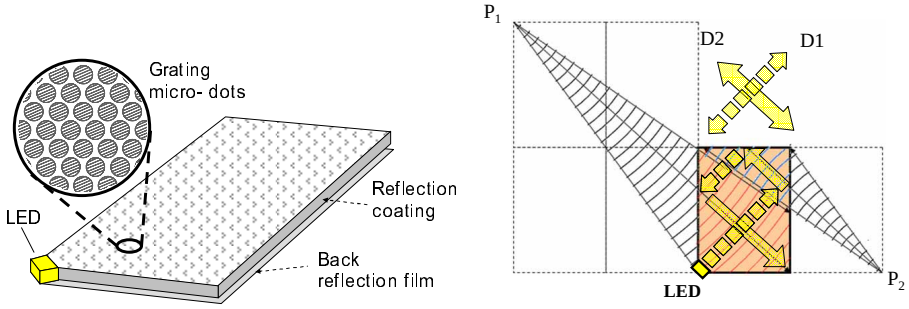

Fig. 1. (a) A schematic diagram of a grating micro-dot patterned LGP under study. (b) Portion of the non-overlapped propagating beam, covering the LGP, which mainly contributes the out-coupling. The P_1 and P_2 are virtual LED sources responsible for two covered regions. Two important directions D1 and D2 are illustrated.

#78558 - $15.00 USD Received 2 January 2007; revised 15 February 2007; accepted 27 February 2007

The LGP, which is made of a polymer material with its bottom and all side walls reflection coated, has a standard 4:3 area aspect ratio. On top of the LGP, an array of grating (with a sinusoidal grating shape) micro-dots is inscribed such that the incident radiation from the LED source can be coupled out as it propagates inside the LGP. Grating micro-dots were two-dimensionally distributed as shown in Fig. 1(a) with their grating-vector orientations and grating depths individually controlled to obtain uniform radiation from the LGP within a narrow luminance angle. An LED source is located at one corner of the LGP and is aligned to have an angle of 48.4^o with respect to the long-sidewall direction such that the center of the radiated beam propagates, reflected by three sidewalls and reaches to the other corner of the LGP as shown by arrows in Fig. 1(b).

The grating diffraction geometry encountered in the design of our LGP structure is schematically illustrated in Fig. 2. A plane wave is incident on a grating from the LGP region with arbitrary azimuth (δ_i, with respect to x axis) and inclination (α_i, with respect to z axis) angles. The incident wave is, then, diffracted by the grating into forward (out-coupling into air) and backward (diffracted back into the LGP) diffraction orders. Under the condition that the azimuth angle $\delta_i \neq 0^o$, the directions of diffracted orders are located in a cone as shown in the figure. Such a general diffraction case is referred to as "conical diffraction." As a diverging LED beam was used and local gratings have arbitrary grating-vector orientations ($\vec{K}$ is along the x direction in the figure, $|K|=2\pi/\Lambda$, and Λ is the grating period) with respect to incoming angular plane wave components in our LGP configuration, conical diffraction is generally occurred. Two important diffraction geometries, relevant to our LGP problem, can be identified. Firstly, in the case $\delta_i=90^o$ ("perfect conical diffraction" case where diffracted orders are located in a circular cone), all forward diffracted orders are evanescent if the incident inclination angle α_i is larger than the critical angle [$\alpha_c=\sin^{-1}(n_1/n_2)$] such that no light is coupled into air. We will refer this grating geometry as the "type 1 diffraction" hereafter. Secondly, when $\delta_i=0^o$, all diffracted orders are located in the x-o-z plane as shown in Fig. 2(b). This grating diffraction geometry is referred to as classical "in-plane diffraction." Under this condition with a sufficiently large incident inclination angle (typically larger than the critical angle), it is possible to make the forward diffracted zero-order evanescent and only the -1st diffracted order to be vertically (in the z-axis direction) out-coupled into air by suitable choice of the grating period. We will refer this grating geometry as the "type 2 diffraction" hereafter. Using these two types of diffraction configurations, we designed the grating micro-dot pattern to extract light from the LGP in a controlled manner.

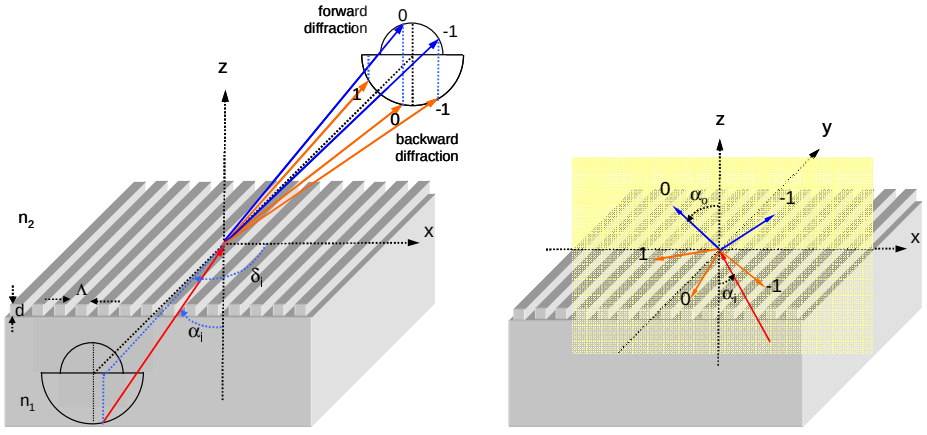

(a) (b)

Fig. 2. Schematic diagrams of (a) conical grating diffraction and (b) classical in-plane grating diffraction.

#78558 - $15.00 USD Received 2 January 2007; revised 15 February 2007; accepted 27 February 2007

For a given LGP configuration in Fig. 1, we designed an out-coupling grating micro-dot pattern as follows. LED-based BLUs are generally suffered by hot spots and light-propagation lines which occur near the LED source region, where incoming light intensity is high [1]. These are caused by imperfections in out-coupling grating pattern due to fabrication limitations. That is, gradually varying low-coupling strength grating pattern is required near the source region to obtain uniform out-coupling intensity distribution, which is difficult to control in fabrication. In order to minimize these unwanted hot spots, orientations of grating vectors inside grating dots are arranged parallel to the D2 direction [D2 direction is graphically defined in Fig. 1(b)] such that propagating beam mainly encounters the type 1 diffraction. Under this condition, initial high-intensity propagating beam propagates inside the LGP with negligible vertical out-coupling until it reaches the first sidewall. With these grating-vector orientations in the grating micro-dot pattern, out-coupling occurs only when the beam is propagating along the direction parallel to the D2 direction (i.e. beams propagating after 1 and 3 sidewall reflections). These beams roughly encounter the type 2 diffraction. Under this situation, portion of the non-overlapped propagating beam, covering the LGP, which mainly contributes the grating out-coupling is identified by two regions as shown in Fig. 1(b). Those are, the upper-right region which is covered by the propagating beam from the LED with a single reflection from the sidewall and the lower-left region which is covered by the beam after three reflections. LED source is assumed as a point source having a Lambertian radiation pattern in this work. In this case the azimuth beam profile in the upper-right and lower-left region can be predicted by two virtual sources P1 and P2 as shown in Fig. 1(b). The covered azimuth angle is in the range 37^o~56^o with respect to the long sidewall direction. Taking into account of the azimuth profile of the propagating beam, grating-vector orientation of each local grating is finely adjusted parallel to the wave front of the propagating beam such that each azimuth angular ray component encounters the type 2 diffraction exactly. With this grating-vector orientation arrangement of local gratings, we can obtain highly directional out-coupled light within a narrow angular width in the D1 direction by minimizing diffraction into that direction.

The grating period (Λ) is an important parameter that determines the direction and the diffraction efficiency of the out-coupled beam. For an LGP BLU, it is desirable to have high-efficiency light extraction in the vertical direction (direction normal to the LGP surface) within a narrow luminance angle. Therefore, the grating period was chosen under the type 2 diffraction configuration to maximize the efficiency of the forward -1^{st} diffracted order coupling out in the direction normal to the LGP surface taking into account of the inclination radiation pattern of the propagating beam. Inside the LGP (with a refractive index of 1.59), the propagating beam from the LED has a Lambertian cosine radiation pattern with an inclination angles of incidence in the range $\alpha_i > 52^o$ due to the total internal reflection condition. Within this incident angle range, we calculated the -1^{st} order forward diffraction efficiencies as functions of the grating period and the inclination incident angle for a sinusoidal grating with a 200 nm grating depth under a green LED (λ=540 nm) illumination. Calculated results (averaged for a TE- and a TM-polarized waves) using a rigorous coupled-wave analysis (RCWA) [9, 10] is given in Fig. 3(a). As can be seen from the figure, forward the -1^{st} order diffraction efficiency is decreased rapidly as the incident inclination angle is increased. For varying grating period, however, diffraction efficiency was negligibly varied in general. Two discontinuous efficiency variation lines can be seen in the figure. These are due to classical Rayleigh anomaly [11]. Within parameter ranges of analysis, two (0^{th} and -1^{st}) forward- and four (0^{th}, $\pm 1^{st}$, and -2^{nd}) backward-diffracted orders were exist, in general. This diffraction efficiency distribution was, then, weighted by the intensity pattern of the LED, which is given in Fig. 3(b). The result shows that, for all grating periods considered, maximum diffraction efficiencies occur near the inclination incident angle of ~60^o. Weighted diffraction efficiencies are shown to be 0 for waves with incident inclination angle smaller than ~52^o, as only waves with inclination angle larger than 52^o can exist inside the LGP due to total internal reflection condition.

#78558 - $15.00 USD Received 2 January 2007; revised 15 February 2007; accepted 27 February 2007

In order to obtain the grating period that maximizes the forward -1st order diffraction efficiency in the vertical direction, we performed another calculation. The solid line in Fig. 4 represents an incident inclination angle that provides maximum forward -1st order diffraction efficiency for a given grating period. The dotted line in the figure represents the required incident inclination angle, calculated from phase-matching condition, for a given period that directs the forward -1st diffracted order along the vertical direction. The crossing point of these two curves corresponds to an optimal condition of an incident angle (α_i=59.5°) and a grating period (Λ=0.394 μm) that maximize the diffraction efficiency of the forward -1st order, which is coupled-out in the vertical direction.

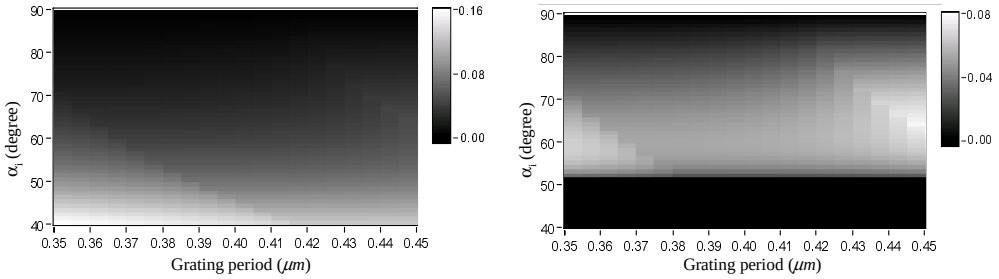

(a) (b)

Fig. 3. (a) Calculated forward -1stdiffraction order as functions of the grating period and the inclination incident angle. (b) Diffraction efficiency weighted by the intensity pattern of the LED.

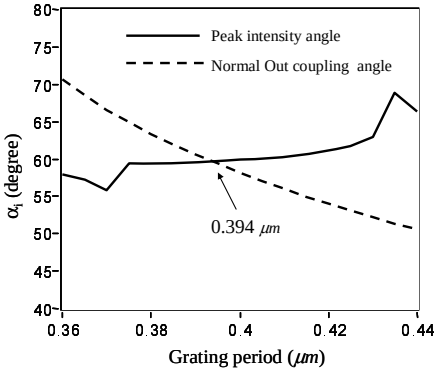

Fig. 4. A grating period that maximize the diffraction efficiency of the forward -1st order, which is coupled-out in the vertical direction.

In order to obtain uniform illumination from the LGP, local gratings should couple out an increasing amount of light as it propagates along the LGP. For controlling out-coupling efficiency of each local grating, considering our fabrication apparatus, we choose to modulate grating depth along the guided-beam path [12]. To optimize the grating-depth modulation pattern in the LGP, we made a simulation tool that can calculate the intensity distribution of the extracted light from the LGP by combining a ray tracing and a rigorous diffraction analysis method. In this simulation tool, an LED source radiation was decomposed into angular ray components in azimuth and inclination angles. Each ray component was, then, traced from the point of an LED source. Upon incidence of a local grating, directions of the forward diffracted and backward-diffracted rays were determined by the phase-matching condition in a general conical grating diffraction configuration. Diffraction efficiency of each

#78558 - $15.00 USD Received 2 January 2007; revised 15 February 2007; accepted 27 February 2007

ray was, then, calculated by an RCWA. Directions and efficiencies of forward (out-coupling) diffracted rays were memorized for that local grating and each backward diffracted ray was traced again. Out-coupling intensity profile from the local grating was, then, obtained by superposition of contributions from all incoming angular ray components on that local grating. Similar calculations were repeated for each local grating all over the LGP.

Typically, 10000 angular ray components (100x100 in azimuth and elevation angles) were initially used to model the angular radiation from an LED source inside the LGP considering the computational resources (i.e. computational time and physical memory). Number of rays to be traced becomes dramatically increases as the initial angular ray component from an LED source experiences a local grating during the propagation along the LGP by the grating diffraction. For example, the azimuth central ray component (propagating along the D1 direction from the LED) with an inclination angle of 60^o experiences 173 grating diffractions as it propagate along the whole LGP. This ray, in general, generates 3 backward diffraction orders (0^{th}, -1^{st}, and -2^{nd}) inside the LGP upon a single grating diffraction, which must be traced on the next step. Theoretically, maximum of 3^{173} rays should be traced for this central ray component during the propagation of the whole LGP. That is, a total of $10000x3^{173}$ rays should be traced including all angular ray components from an LED. Tracing of this large rays is computationally too demanding. In order to make the ray tracing problem manageable, we only traced local diffracted rays with relatively large cumulative diffraction efficiency (>1% of the incident angular ray component intensity). This substantially reduces the total number of traced rays. After experiencing small number of gratings as the initial angular ray component propagates, only the 0^{th} and -1^{st} orders have significant cumulative diffraction efficiencies and survived, in general. With this implementation, it took about 40 minutes to obtain the intensity pattern of the whole LGP using a personal computer (2GHz AMD CPU with a 2GB memory). The detailed descriptions of the implementation and computational performance of the simulation model will be presented in a separate paper.

This simulation tool was used to check the luminance uniformity of the LGP in the design stage of grating-depth modulation in the grating micro-dot pattern. Optimized grating-modulation pattern for uniform intensity distribution in out-coupled light was obtained as follows. We started with the same grating depth of 100 nm for every local grating micro-dots and calculated the extracted light distribution from the LGP. After analyzing the resulting intensity distribution, depth of each local grating was adjusted from the current value by

$$\Delta d = \begin{cases} \dfrac{I - I_{avg}}{I_{\max} - I_{avg}}(d - d_{\min}), I < I_{avg} \\ \dfrac{I_{avg} - I}{I_{avg} - I_{\min}}(d_{\max} - d), I > I_{avg} \end{cases} \quad (1)$$

where I is the current intensity at a local grating under consideration, I_{max}, I_{min}, and I_{avg} are maximum, minimum, and average intensity in the whole LGP. The d_{max} and d_{min} are maximum and minimum grating depths controllable in the fabrication stage and were given by 70nm and 200nm, respectively. Iterative radiation profile simulations were performed for adjusted grating-depth modulation patterns until desired intensity uniformity from the LGP was achieved. Typically 8 iterations were enough to ensure luminance uniformity better than 85%. For an LGP with a dimension of 30mm x 40mm x 0.6mm illuminated by a green LED (λ=540nm), obtained grating-depth modulation profile and corresponding output intensity distribution is given in Figs. 5(a) and (b), respectively. In these figures, an LED is located at (0, 0). The resulting intensity pattern of extracted light shows no noticeable hot spots and intensity uniformity was better than ~85% for this LGP design. In the simulation of obtaining intensity distribution in Fig. 5 (b), whole LGP area was divided by 12x16 grid cells (cell resolution of 2.5mmx2.5mm) and average intensity within these grid cells were calculated and compared.

#78558 - $15.00 USD Received 2 January 2007; revised 15 February 2007; accepted 27 February 2007

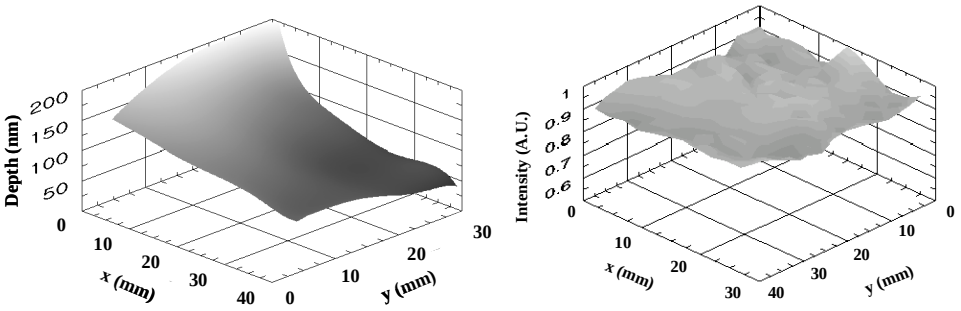

(a) (b)

Fig. 5. (a) Optimized grating-depth distribution and (b) corresponding normalized out-coupling intensity distribution from the LGP.

Figure 6(a) shows calculated luminance angular distribution of the extracted light. The luminance angles (FWHM) were found to be ~2° and ~10° along the D1 (solid line) and D2 (dotted line) direction, respectively. Luminance angles along the D1 and D2 direction [shown at the bottom of Fig. 6 (a)] refers to a cross-sectional angular distribution (passing the LGP surface normal) along the D1 and D2 directions. The luminance angle in the D1 direction mainly depends on the LED's azimuth radiation angle range ($\Delta\theta_{az}=19^{o}$), where out-coupling is controlled by grating-vector orientation arrangement of the LGP as shown in Fig. 1 (b), and corresponding azimuth intensity pattern of the LED. Due to the small angular range involved, luminance angle in this direction is also small. The luminance angle in the D2 direction, on the other hand, depends on the inclination angle range of the LED radiation in side the LGP (in terms of grating incident angle, it is $\alpha_i=52^{o}\sim90^{o}$) and corresponding intensity radiation pattern of the LED. Due to the in-plane diffraction involved in this case, the luminance angle in this direction is broader than in the D1 direction. Narrow luminance angles (especially in

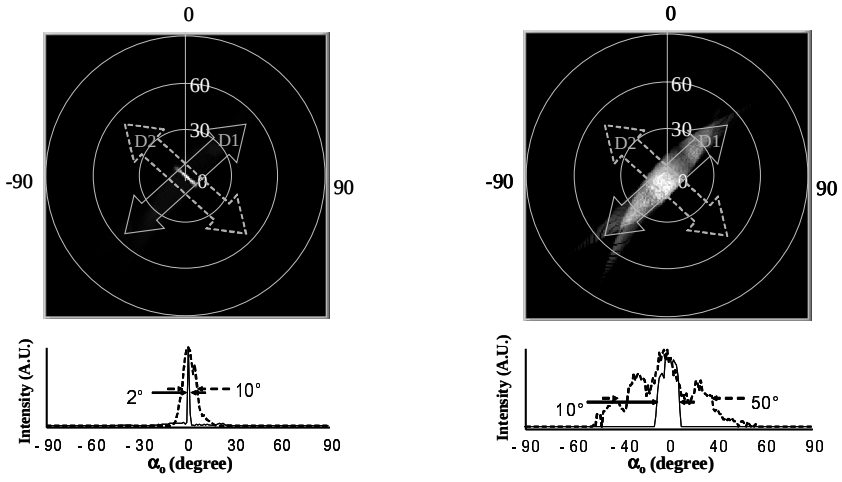

(a) (b)

Fig. 6. Luminance angular distributions when each local grating-vector orientation is (a) aligned with respect to LED's azimuth beam profile and (b) fixed to D2 directions.

#78558 - $15.00 USD Received 2 January 2007; revised 15 February 2007; accepted 27 February 2007

D1 direction) were able to be obtained due to the fact that grating-vector orientations of most local gratings are finely aligned with respect to LED's azimuth radiation pattern such that almost no beam propagating along the D1 direction can couple out. Without such a grating-vector orientation alignment, as in the case of an LGP with every local grating has grating vector along the D2 direction for example, substantial amount of beam can couple out from the LGP as the beam propagates along the D1 direction by experiencing a general conical grating diffraction. This makes a substantial broadening of the luminance angle in the D1 direction, which was calculated to be ~50^o as shown in Fig. 6(b). Due to the same reason, luminance angle in the D2 direction is broadened by 5 times (~10^o) in this grating orientation arrangement as shown in the figure.

3. Device fabrication and evaluation

A grating micro-dot patterned LGP was fabricated and experimentally evaluated. A ~2.1 μm-thick photoresist (Clariant AZ P4210) layer was spin-coated on a 4-inch glass substrate and was soft-baked on a 90^{o}C hot plate for 30 minutes. Grating micro-dots (with a sinusoidal grating profile) were sequentially recorded on the photoresist-coated substrate using a dot-matrix holographic interferometer setup as shown in Fig. 7. Total 132 × 86 micro-grating dots were recorded on the substrate covering a rectangular area of 30 mm × 40 mm. In this setup, an Ar+ laser (λ=458 nm) was spatially filtered and focused by a focusing lens. The focused beam was divided into two beams by a beam splitter and, then, combined again by two mirrors to form a focused interference pattern on the substrate surface. Optical powers of both beams were well balanced to have ~5mW by a variable attenuator. The recording angle (θ) was ~35.54^o to obtain a grating period of ~394 nm. The substrate was mounted on motorized x-y-ϕ stages as shown in the figure. A film coated with UV absorber was placed between the substrate and the stage surfaces to minimize the effect of back reflection during the exposure. The location of each grating micro-dot was controlled by two motorized linear stages with a ~0.25 μm resolution. The dot-matrix holographic interferometer setup used in this work was mainly different from that proposed by Lee et al. [8] in the way to control grating-vector orientation. While an optical head, including major optical components forming an interferometer was rotated in their setup, the substrate was rotated using a rotation stage (with a 1^o resolution) in our case to control the orientation of the grating vector. This approach may be simpler and more robust in recording large amount of grating micro-dots in our LGP. The grating-depth control in the array was achieved by controlling laser exposure time using an electronic shutter. The whole dot-matrix holographic recording process was controlled by a computer.

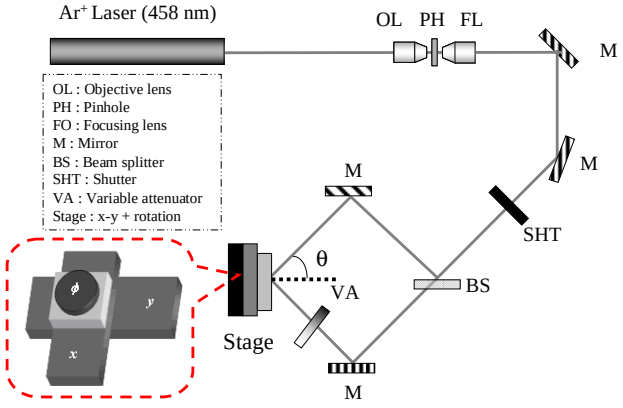

Fig. 7. The schematic diagram of a dot-matrix holographic interferometer setup used in the fabrication of a grating micro-dot pattern.

#78558 - $15.00 USD Received 2 January 2007; revised 15 February 2007; accepted 27 February 2007

Figure 8(a) shows an optical microscope image of a typical grating micro-dot pattern having a dot spacing of ~500 μm fabricated by the above-mentioned dot-matrix holographic interferometer setup. As might be seen in the figure, the gratings inside a dot have non-uniform grating depths. This is due to the fact that two interfering focused beams have Gaussian-like beam profiles rather than uniform intensity profiles. Corresponding scanning electron micrograph (SEM) near the central part of the dot is given in Fig. 8(b) showing a sinusoidal grating with a period of ~395 nm.

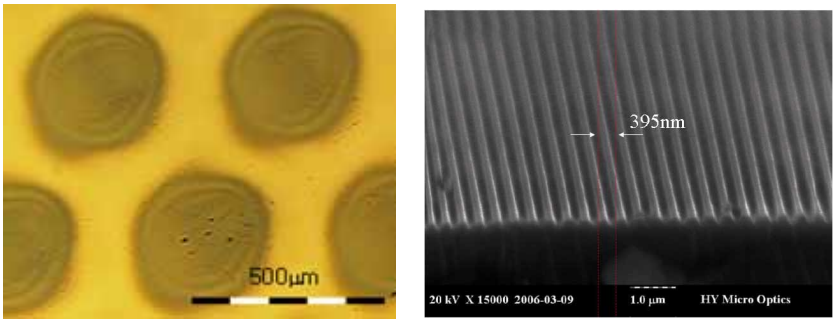

(a) (b)

Fig. 8. (a) An optical microscope image of the micro-grating dots recorded in photoresist. (b) An SEM picture of the grating inside a micro-grating dot.

To see the grating-depth controllability using our interferometer setup, we fabricated and tested several holographically recorded grating micro-dot patterns with varying laser exposure time. For laser exposure times of 100, 125, 150, and 200 ms, fabricated grating depths were found to be ~93, ~174, ~201 and ~225 nm, respectively, which can be seen from SEM pictures given in Fig. 9.

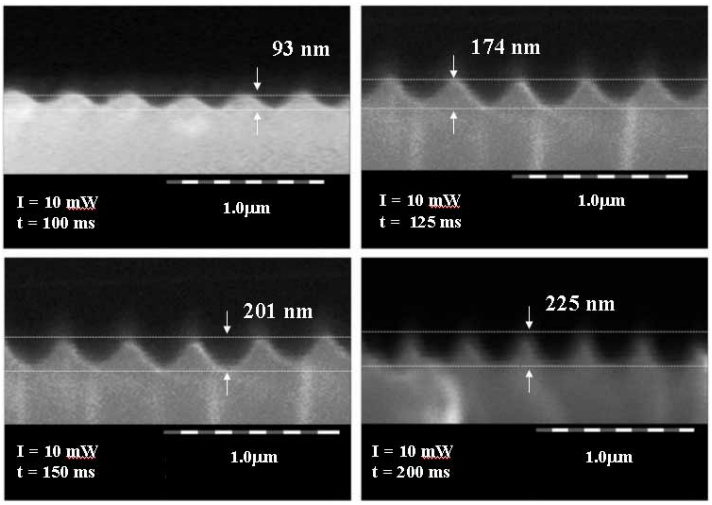

Fig. 9. SEM pictures of the fabricated gratings with varying laser exposure times.

#78558 - $15.00 USD Received 2 January 2007; revised 15 February 2007; accepted 27 February 2007

To characterize the fabricated grating micro-dot patterns, we measured the backward -1st order diffraction efficiencies using a TM-polarized HeNe laser (λ=632.8 nm) at an incident angle of 45° as shown in Fig. 10(a). Comparison of the theoretically calculated diffraction efficiencies and measured values are given in Fig. 10(b). Measured -1st order backward diffraction efficiencies (square dots) were shown to be lower than theoretical calculations (solid line) assuming all area of the sample was filled with a linear grating. This is due to the fact that fabricated grating dots do not cover all area of sample as shown in Fig. 8(a). Grating non-uniformity inside the micro-dot may additionally affect this discrepancy. We introduced an effective dot fill factor (area portion of the unit cell the dot occupied) to take into account of this discrepancy. When the calculated diffraction efficiencies were weighted by the effective dot fill factor of ~0.44, the measured efficiencies and fitted results were found to agree. Corresponding effective dot size is calculated to be ~350 μm.

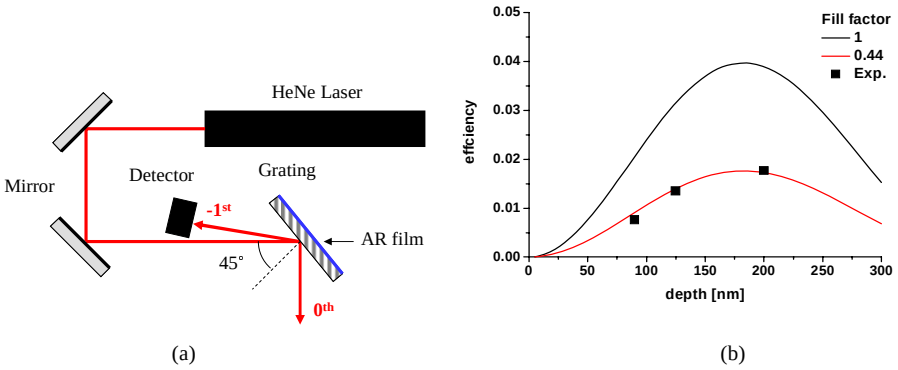

Fig. 10. (a) A schematic of the diffraction efficiency measurement. (b) Comparison of efficiencies of -1st order backward diffracted order as a function of the grating depth obtained by theoretical calculation and experimental measurements.

Final LGP device was made by UV embossing replication process [11]. Fabricated photoresist grating micro-dot array pattern was first transferred to a PDMS molding by contact imprinting followed by thermal curing. Using the PDMS stamper, we made a replica of the grating micro-dot pattern on a polycarbonate light guide plate (30 mm x 40 mm x 0.6 mm) coated with UV epoxy (Norland Optical Adhesive 61) by direct contact imprinting and successive UV curing for ~5 min. Both the polycarbonate substrate and the UV epoxy used have similar refractive index of ~1.59. Side reflectors were made by gluing pieces of aluminum coated sheet using an adhesive. Final polycarbonate LGP was placed on top of an aluminum-coated sheet for bottom reflection. Figure 11(a) shows a CCD camera image of the fabricated LGP. A white LED radiation was coupled into the LGP by a corner butt-coupling. The circular shaped image in the figure is a camera lens image reflected by the bottom reflection sheet. Figure 11(b) shows corresponding measured output light distribution. The measured intensity uniformity over the LGP surface was ~62%, which is somewhat lower than designed value of ~85%. Two main intensity non-uniformities can be seen from Fig. 11. Firstly, a bright line pattern exists along the diagonal direction. This line corresponds to the intersection between two virtual sources as shown in the Fig. 1 (b). As the grating-vector orientation pattern in the LGP was designed based on portion of the LED's azimuth radiation pattern as defined in Fig. 1 (b), azimuth angular ray components beyond this angle range may out-couple the incoming ray in an uncontrolled manner. Although minimization of intensity non-uniformity due to this effect was considered in the design stage of thickness-modulation, line-intensity pattern was still observed because substantial out-couplings occur from both virtual sources along this line and summed. This may be due to imprecise control of the

#78558 - $15.00 USD Received 2 January 2007; revised 15 February 2007; accepted 27 February 2007

grating depth pattern in the fabrication stage. Another bright region was shown to exist at the lower right corner of the LGP. This may be due to the fact that out-coupling by fabricated local gratings in the LGP was not sufficient. That is, after propagating the whole LGP (at the right corner of the LGP), light energy was not fully coupled out such that remaining energy was additionally coupled-out in this region after reflection from the lower right corner reflectors.

These non-uniformities are basically originated from both the inaccuracy of the simulation model and the fabrication errors. Firstly, not only the grating depth but spot size variation in the recorded micro-grating dot was observed when we varied the exposure time. Although we try to fit this effect by introducing an effective dot fill factor (equal to a constant value of 0.44 to make the simulation computationally easy) in the design of the grating micro-dot pattern, this parameter does not seem to be well modeled as a constant value as shown in Fig. 10(b). Secondly, the out-coupling grating pattern was designed with parameter optimizations at a green LED wavelength. Under the white LED illumination such as in our experiment, diffraction characteristic may be slightly different. Thirdly, fabrication error in the thickness-modulation pattern may be due, in part, to the Ar+ laser instability during the exposure of whole LGP area (4~5 hours). Additional fabrication errors include imperfections in side and back reflectors.

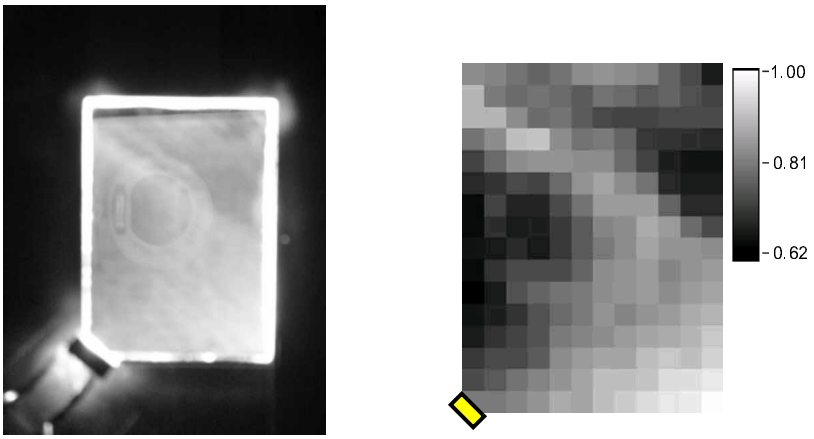

(a) (b)

Fig. 11. (a) A camera image of the fabricated LGP and (b) corresponding intensity distributions.

Luminance angles (FWHM) of the out-coupled light were measured by EzContrast 160 (ELDIM). Measured angles were ~8^{o} and ~20^{o} in the D1 and D2 directions, respectively, as shown in Figs. 12 (a) and (b). These values are a little bit larger than theoretically estimated values. Broadening of luminance angles may come from following reasons. Firstly, the grating micro-dot pattern was designed considering only main portion (39^{o}~52^{o}) of the azimuth beam pattern. The rest portion of the beam, although relatively weak, may cause conical diffraction into undesirable directions resulting in luminance angular broadening. Use of a white LED rather than a green LED in the experiment may be another reason for this angular broadening (especially in the D2 direction) due to chromatic dispersion under in-plane diffraction configuration. In order to see this, we performed a simulation using three LEDs (R: 640 nm, G: 540 nm, and B: 440 nm) to obtain the intensity distribution of extracted light from the LGP designed for a green LED. Calculated results in Figs. 12 (c) and (d) show angular broadening of ~1.5 time in the D2 direction without angular broadening in the D1 direction. Diffraction due to periodic distribution of micro-dots and imperfections in side and back reflectors may also affect this luminance angular broadening.

#78558 - $15.00 USD Received 2 January 2007; revised 15 February 2007; accepted 27 February 2007

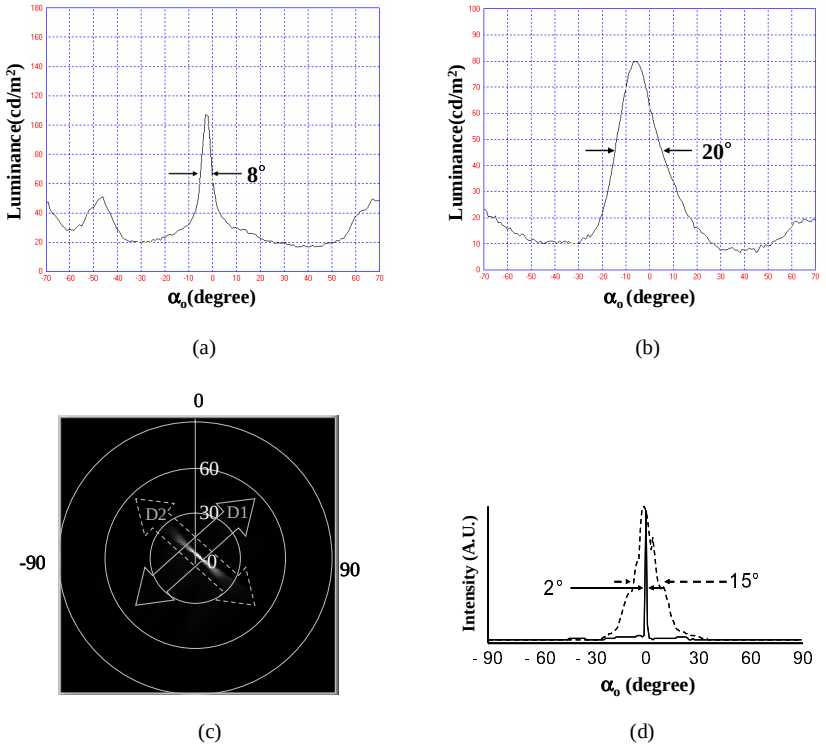

Fig. 12. Measured luminance angular distributions in the direction of (a) D_1, (b) D_2. (c) Simulated luminance angular distribution using a white LED and (d) cross-sectional view of those in the direction of D_1 and D_2.

4. Summary and conclusion

In conclusion, a novel LED backlight unit implementing grating micro-dot patterned LGP was proposed. By applying optimized grating-depth modulation in the array pattern, uniform out-coupled light distribution was achieved without recognizable hot spots near the LED source. Additionally narrow luminance angular distribution was obtained by fine tuning the grating-vector orientation of each local grating with respect to the azimuth radiation beam profile of the LED. This may eliminate the conventionally used prism sheets such that the proposed grating dot patterned LGP can be a simple and low cost solution for LED back light units. Such an LGP was fabricated using a dot-matrix holographic lithography and a UV embossing replication. Fabricated LGP showed ~62% intensity uniformity within narrow (~8^o and ~20^o) luminance angles. The combined processes of the dot-matrix holographic lithography mastering and UV replication may be a flexible, cost effective, and promising method to fabricate large arrays of micro-gratings with arbitrarily controlled grating orientation and depth.

Acknowledgments

This work was supported in part by the Engineering Research Center Grant No. R11-2003-022-01001-0 (2006). The authors are grateful for useful comments to improve this paper by one of the reviewers.

#78558 - $15.00 USD Received 2 January 2007; revised 15 February 2007; accepted 27 February 2007